NIH Public Access
Author Manuscript
Magn Reson Med. Author manuscript; available in PMC 2009 July 1.

Published in final edited form as:
Magn Reson Med. 2008 July ; 60(1): 14–20. doi:10.1002/mrm.21651.

In Vivo MRI Using Real-Time Production of Hyperpolarized ^{129}Xe

Bastiaan Driehuys[1], **Jim Pollaro**[2], and **Gary P. Cofer**[1]

[1]Center for In Vivo Microscopy, Department of Radiology, Duke University Medical Center, Durham, NC

[2] Advanced Imaging Research Center, Oregon Health Sciences Center, Portland OR

Abstract

MR imaging of hyperpolarized (HP) nuclei is challenging because they are typically delivered in a single dose of non-renewable magnetization, from which the entire image must be derived. This problem can be overcome with HP ^{129}Xe, which can be produced sufficiently rapidly to deliver in dilute form (1%) continuously and on-demand. We demonstrate real-time *in vivo* delivery of HP ^{129}Xe mixture to rats, a capability we now routinely use for setting frequency, transmitter gain, shimming, testing pulse sequences, scout imaging, and spectroscopy. Compared to images acquired using conventional fully concentrated ^{129}Xe, real-time ^{129}Xe images have 26-fold less signal, but clearly depict ventilation abnormalities. Real-time ^{129}Xe MRI could be useful for time-course studies involving acute injury or response to treatment. Ultimately, real-time ^{129}Xe MRI could be done with more highly concentrated ^{129}Xe, which could increase SNR by 100 relative to these results to enable a new class of gas imaging applications.

Keywords

Hyperpolarized ^{129}Xe; Continuous Flow; Ventilation

INTRODUCTION

Magnetic resonance imaging (MRI) using hyperpolarized (HP) nuclei (^{3}He, ^{129}Xe, ^{13}C, ^{15}N) presents enormous opportunities for novel functional and metabolic imaging (1-4). However, a major challenge of these agents is their non-renewable magnetization, which requires careful experiment design to derive all the desired information from a single dose. This limited signal availability complicates even mundane activities such as pre-scanning, reduces SNR by requiring small flip angles to be used, but most importantly narrows the scope of the science that can be explored. These limitations can be overcome by HP ^{129}Xe, whose polarization physics is intrinsically rapid. Moreover, since ^{129}Xe is a gaseous agent that is delivered and excreted by ventilation there is, in principle, no limit to the amount of gas that can be administered over time. This unique opportunity stands in stark contrast to all other contrast agents and has yet to be fully exploited. The utility of continuous HP ^{129}Xe delivery has already been embraced for *in vitro* ^{129}Xe NMR spectroscopy applications (5), but not yet for *in vivo* imaging.

The gaseous agents ^{129}Xe and ^{3}He are most commonly hyperpolarized through the well-known spin exchange optical pumping (SEOP) method (1,6). SEOP is a 3-step process whereby angular momentum is transferred from laser photons to alkali metal electron spins

Correspondence: Bastiaan Driehuys, Ph.D. Center for In Vivo Microscopy Box 3302, Duke University Medical Center Durham, NC 27710 (TEL) 919−684−7786 (FAX) 919−684−7122 (E-mail) driehuys@orion.duhs.duke.edu.

NIH-PA Author Manuscript
NIH-PA Author Manuscript
NIH-PA Author Manuscript

NIH-PA Author Manuscript

NIH-PA Author Manuscript

NIH-PA Author Manuscript

and then to noble gas nuclei. Typically the alkali metal Rubdium (Rb) is used because its 795nm D_1 optical pumping resonance is readily accessible by commercially available high-power lasers. Compared to ^{3}He, hyperpolarization of ^{129}Xe is intrinsically rapid because the large positive charge of the Xe nucleus draws in the alkali valence electron wave function (7), and thereby intensifies the Rb-^{129}Xe interaction. For this reason, the spin exchange cross-section for binary Rb-^{129}Xe collisions (8) is 3284-fold larger than for Rb-^{3}He collisions (9), a ratio that is enhanced yet further by the formation of Rb-^{129}Xe molecules at low pressures (10). The larger ^{129}Xe spin exchange cross-section translates directly into faster spin exchange rates for a given vapor pressure of alkali metal. For example at 200°C, Rb-^{3}He spin exchange occurs with a time constant of 4.5 hours, whereas binary Rb-^{129}Xe spin exchange occurs with a 2.5-second time constant. Unfortunately, the strong Rb-^{129}Xe interaction comes at a price — namely, the cross section for binary Xe-Rb collisions that destroy the Rb spin (11) is 3944-times larger than for He-Rb collisions (9). Therefore ^{129}Xe must typically be polarized in dilute mixtures containing only 1% Xe. The balance of the mixture contains 10% nitrogen and 89% helium buffer gases to quench fluorescence (12) and to sufficiently broaden the Rb absorption (13). These constraints have led to ^{129}Xe polarizer designs wherein dilute ^{129}Xe is rapidly polarized in a continuously flowing gas stream and is then subsequently concentrated by cryogenic accumulation (14). This process over time generates a sufficient quantity of frozen HP ^{129}Xe, which can then be thawed and delivered for imaging. However, these batches can take many minutes or even hours to accumulate and therefore sacrifice the inherent signal continuity of HP ^{129}Xe. To re-gain signal continuity, we forego the cryogenic accumulation step and reduce the pressure of the flowing ^{129}Xe to physiologic levels, which makes it possible to deliver the dilute ^{129}Xe mixtures directly and continuously to the animal.

The flow rate of ^{129}Xe mixture that is necessary to ventilate an animal can be estimated by allometric scaling (15) according to $\dot{V}_r = 6.32M^{0.80}$, where $\dot{V}_r$ is the ventilation rate in ml/s, and M is the mass in kg. Hence, a rat with M =250 g must be ventilated at a rate of 125ml/min and assuming that 21% of this flow consists of oxygen requires the ^{129}Xe mixture to be delivered at a rate of 99 ml/min. This flow rate is readily delivered by any current small-scale ^{129}Xe polarizer, such as the one in our laboratory that commonly employs flows of 500 − 2000ml/min (14).

METHODS AND RESULTS

All ^{129}Xe polarization was carried out using a modified prototype continuous-flow commercial polarizer (IGI.9800.Xe, MITI, Durham, NC). The polarizer could be operated either in its normal mode to generate a batch of concentrated HP ^{129}Xe by cryogenic accumulation, or in real-time mode to continuously deliver the dilute 1% ^{129}Xe mixture to the animal. The polarizer was modified as shown in Figure 1 by removing the cryogenic accumulation stage and routing the HP gas mixture directly from the output of the optical cell into a pressure regulator (PR-1−2214, Partek, Tuscon, AZ) that was constructed entirely out of Teflon. This regulator reduced the gas pressure from the 4−6 atm used during hyperpolarization, down to physiologic pressures suitable for delivery to an animal. This regulator was selected because its all-Teflon construction was expected to better retain ^{129}Xe polarization compared to conventional regulators containing steel components. The regulator's low-pressure output was routed using ¼” Perfluoroalkoxy (PFA) tubing (PFA-T4−047−100, Raleigh Valve & Fitting, Raleigh, NC) to an HP-gas compatible ventilator (16) where it replaced the typical Tedlar bag in a pressurized cylinder (17) that has become the standard for small animal HP gas delivery.

The ventilator operated at 60 breaths per minute and delivered a constant volume of O_2 per breath (18), which we set to 0.18 ml per 100 grams of animal body weight. The balance of

NIH-PA Author Manuscript

NIH-PA Author Manuscript

NIH-PA Author Manuscript

the tidal volume was made up by a separate line delivering 0.66 ml per 100 gram of N_2. The N_2 line was substituted by HP ^{129}Xe mixture during imaging. The ^{129}Xe mixture delivery was controlled by a pneumatic Teflon valve (Model PV-1−1134, Partek, Tuscon AZ) that was selected for fast switching and for polarization retention. During HP gas/O_2 ventilation, the tidal volume was kept the same as during normal ventilation by adjusting the HP gas regulator to attain the same peak inspiration pressure (PIP). Pressure was recorded using an MR-compatible pressure transducer (XFGM-6, Fujikara/Servoflo, Lexington, MA) located ~3 cm from the rat's tracheal tube.

A final consideration to ensure consistent HP ^{129}Xe mixture delivery was to create a small bypass flow (100 ml/min) from the output of the HP gas regulator to a needle valve that vented to the atmosphere. This bypass flow ensured that the ^{129}Xe mixture continually flowed through the optical cell and outlet tubing leading to the ventilator, thereby eliminating pressure fluctuations and ensuring seamless switching from normal breathing to HP ^{129}Xe delivery.

MR Imaging Hardware

Images and spectra were acquired on a 2.0 T horizontal 30 cm clear bore magnet (Oxford Instruments, Oxford, UK) with shielded gradients (18 G/cm), controlled by a GE EXCITE 12.0 console (GE Healthcare, Milwaukee, WI). The scanner was interfaced to a 23.66 MHz linear birdcage coil (8 cm long, 7 cm diameter) by an integrated transmit/receive switch with 31 dB gain preamplifier (Nova Medical, Wilmington, MA). The frequency of the scanner was modified from its intrinsic 63.86 MHz value to 23.66 MHz using an up-down converter (Cummings Electronics Labs, North Andover, MA).

Characterization of ^{129}Xe Polarization and Retention

Although we routinely use both natural and enriched ^{129}Xe for our studies, all images and spectra shown in this communication were acquired using ^{129}Xe enriched to 83% (Spectra Gases, Alpha, NJ). We first characterized the ^{129}Xe polarization and retention during continuous flow delivery by directing the ^{129}Xe mixture from the polarizer, through the regulator and into a spiral phantom constructed of PFA tubing (Figure 2A). The regulator was set to its maximum output pressure of 3.54 atm, which resulted in sufficient ^{129}Xe signal at a mixture flow rate of 0.2 SLM to acquire a 3D image of the phantom (Figure 2B). The image was acquired using a radial sequence with flip=10°, BW=8 kHz, TR/TE=25/0.3 ms, 46080 frames, matrix=128^3, FOV=12×12×12 cm^3 for an isotropic resolution of $(0.94\ mm)^3$. This example shows the utility of real-time ^{129}Xe MRI for testing pulse sequences.

To quantify ^{129}Xe polarization as a function of mixture flow rate and to determine whether inserting the regulator caused any polarization loss, the signal in the phantom was quantitatively probed by 1D spectroscopy using a chemical shift imaging (CSI) pre-scan routine employing a 500 μs long, 5° hard pulse with TR=1 s. The ^{129}Xe mixture flow rate was varied from 0.1 SLM to 3 SLM, and at each flow rate, ^{129}Xe signal was allowed to equilibrate in the phantom, then the flow was stopped, and a signal was recorded. Signal versus flow curves were acquired both with the regulator in line (3.54 atm) and with the regulator removed (pressure=4.65 atm). The corresponding ^{129}Xe polarization was subsequently calibrated by filling the phantom with a known pressure (~6 atm) of 50% natural xenon, and 50% O_2 and probing the signal with 90° hard pulses. The paramagnetic oxygen ensured that ^{129}Xe would relax with T_1~1.5 s (19) to thermal equilibrium values. Thermal ^{129}Xe signal was detectable in a single shot, but 64 averages were collected to improve SNR. The thermal ^{129}Xe signal was then used to calibrate the HP ^{129}Xe signal in conjunction with suitable corrections for ^{129}Xe concentration differences, flip angles, and incomplete thermal relaxation. The resulting ^{129}Xe polarization is plotted as a function of

NIH-PA Author Manuscript

NIH-PA Author Manuscript

NIH-PA Author Manuscript

flow rate in Figure 3 and data were fit to the expression $P(F) = P_0(1 - e^{-F_{crit}/F})$ to yield a peak polarization level of 25±1% without the regulator and 25.8±1% with the regulator. For both conditions F_{crit}=1.35±0.1 SLM. The somewhat low polarization and production rate are due to the deteriorating power (49 W) and line-width (2.5 nm FWHM) of our laser. However, these results clearly indicate that ^{129}Xe polarization is unaffected by the regulator and that the ^{129}Xe mixture production rate is more than sufficient to continuously deliver 25% polarized ^{129}Xe mixture to a rat.

Animal Preparation

The *in vivo* results reported in this communication were gathered from 30 different imaging studies that employed real-time ^{129}Xe delivery in rats. Three of the rats had unilateral pulmonary fibrosis in the left (n=2) or right (n=1) lung from instillation of Bleomycin, as described in reference (2). The rats were Fischer 344 (Charles River, Raleigh, NC) weighing 170−200g and they were anesthetized by intraperitoneal (IP) injections of 56 mg/kg ketamine (Ketaset, Wyeth, Madison, NJ) and 2.8 mg/kg diazepam (Abbott Labs, Chicago, IL). Anesthesia was maintained with periodic injections of ketamine and diazepam at ¼ the initial dose. Rats were perorally intubated using a 16-gauge catheter (Sherwood Medical) and ventilated in the supine position at a rate of 60 breaths/min and a tidal volume of 1.25 ml per 100 g. A single breath consisted of a 250 ms inspiration, 200 ms breath-hold, and a 550 ms passive exhalation. At the start of the breath-hold, the ventilator triggered the MRI scanner to start the acquisition so that images or spectra were acquired without respiratory motion. During all studies, the rat's airway pressure, temperature, and ECG were continuously monitored. Body temperature was controlled by warm air circulating through the bore of the magnet.

^{129}Xe Polarization

For real-time imaging, the ^{129}Xe mixture flow rate through the polarizer was set using a bypass flow of roughly 100 ml/min. Thus, during ^{129}Xe delivery to the animal, the total ^{129}Xe mixture flow rate was 200 ml/min and ^{129}Xe polarization was ~ 25%. To alternatively polarize a batch of concentrated ^{129}Xe, the ^{129}Xe mixture flow rate was set to ~1200 ml/min and cryogenic accumulation continued for roughly 45 min to yield 540 ml of concentrated Xe, of which 60 ml was used for gas-phase imaging, and the remainder was used for other studies. The ^{129}Xe polarization obtained from batch production was 8−10% as determined using a 24 kHz pulsed NMR circuit calibrated by a portable polarization transfer standard (20). The approximately 3-fold lower polarization from batch accumulation relative to real-time delivery results from three factors. First, the 1.2 SLM flow rate during batch accumulation gives a lower ^{129}Xe polarization (~17.5%) than at 0.2 SLM (~25%). Second, longitudinal relaxation of the frozen ^{129}Xe (21) during the 45-minute accumulation will reduce ^{129}Xe polarization to ~15%. Third, in our system, ^{129}Xe experiences roughly 33% polarization loss during the freeze/thaw cycle. These factors mean that the instantaneous magnetization available during real-time ^{129}Xe delivery is only 33-times lower than during batch production, even though the ^{129}Xe concentration is 100-times lower.

Pre-Scanning and Signal Stability during Real-Time ^{129}Xe Delivery

Once the animal was in the magnet, the ^{129}Xe polarizer was started at a bypass flow of 0.1 SLM, ^{129}Xe mixture delivery was initiated, and the HP gas regulator was adjusted to match the animal's peak inspiratory pressure (PIP) to that observed during normal ventilation. Within a few seconds, the ^{129}Xe signal became detectable during pre-scan. For pre-scanning, we used the FID CSI sequence interface because it permits acquisitions to be gated to the ventilator, pre-scan signals can be saved if desired, and the ^{129}Xe signal can be evaluated in a phase-sensitive manner, making it very straightforward to determine the 180°

NIH-PA Author Manuscript

NIH-PA Author Manuscript

NIH-PA Author Manuscript

pulse from which all other transmit gain settings can be calculated. A pre-scan screen capture is seen in Figure 4 showing the *in vivo* HP ^{129}Xe signal that was obtained after a single 90° pulse. Since this signal was updated every breath, it was more than sufficient for shimming, setting the transmit frequency, and transmit gain.

To determine the stability of real-time ^{129}Xe delivery, we made long-term recordings of the animal's PIP, and acquired ^{129}Xe signals every 5−10 minutes. A plot of PIP and ^{129}Xe signal recorded over a period of 160 min is shown in Figure 5. For this plot, normal ventilation was recorded for 4 min and then HP ^{129}Xe was started and the regulator was adjusted to maintain a PIP of ~10 cm H_2O. The pressure remained constant with only a very slight rise over the course of 80 minutes. Then the HP ^{129}Xe was stopped, the animal was given a deep inspiration to clear any lung atelectasis and HP gas was started again. ^{129}Xe signal returned to its previous value within 10−15 seconds. The pressure and signal remained stable until about t=140 minutes when both began to rise slightly and HP ^{129}Xe was stopped and the animal was given another resetting breath. The extraordinary stability of signal suggests that images or spectra could be acquired over many hours if desired. Some rats were ventilated on ^{129}Xe mixture for as long as 5 hours without complications.

Comparison of Real-Time versus Batch-Delivered ^{129}Xe MRI

Radially acquired images using real-time ^{129}Xe delivery were compared to those from batch ^{129}Xe delivery. Radial imaging is used in our laboratory for high-resolution HP gas imaging because such sequences protect against the effects of diffusion-induced attenuation, which can become extreme at microscopic resolution (22). All acquisitions were done without slice selection gradients and employed a 3-lobe sinc pulse excitation lasting 1.2ms (3.3 kHz bandwidth) to avoid excitation of the dissolved phase ^{129}Xe. For real-time imaging, we used FOV=7 cm, matrix=64×64, 4kHz bandwidth (BW), 200 radial projections, acquired 4 views per breath with TR/TE=50/0.83 and a variable flip angle that incremented from 30° to 90° (23). These images had a Nyquist-limited resolution of 1.1×1.1mm^2, took 50 seconds to acquire, and consumed approximately 0.75 ml of xenon. For comparison, high-resolution 2D ventilation images were acquired in the same animals during delivery of fully concentrated ^{129}Xe. These images employed 2D radial encoding with FOV=4.0 cm, matrix=128×128, TR/TE=20/0.83 ms, BW=8 kHz, 400 radial projections, acquired 10 views per breath, with a variable flip angle incrementing from α_1=18° to α_{10}=90°. The images had a Nyquist-limited resolution of 312×312 μm^2, took 40 seconds to acquire, and consumed 60 ml of xenon.

A comparison of 5 rats that underwent imaging with both batch and real-time ^{129}Xe delivery is shown in Figure 6. Comparing batch versus real-time, we achieved resolutions of 0.31×0.31mm^2 with SNR of 10−21 in the distal lung versus 1.09×1.09mm^2 with SNR of 7.5−15 in the distal lung, reflecting on average a factor of 26 signal difference between the two operating modes when slight differences in image acquisition time (50 s and 40 s) were accounted for. This is consistent with expectations of an instantaneous 33-fold signal difference based on polarization and ^{129}Xe concentration arguments already outlined. The slightly better than expected SNR from real-time ^{129}Xe images could have resulted from less diffusion-induced signal attenuation incurred at the lower image resolution (22). Importantly, the real-time images were of sufficient quality to delineate the major airways and to observe the reduced ventilation (arrows) in animals that had received bleomycin instillation.

^{129}Xe Spectroscopy Studies

As an example of using real-time ^{129}Xe delivery to probe animal physiology beyond the airspaces, we acquired ^{129}Xe spectra to measure alveolar capillary gas transfer efficiency

NIH-PA Author Manuscript

NIH-PA Author Manuscript

NIH-PA Author Manuscript

(2,24,25). This type of spectroscopy takes advantage of the large ^{129}Xe chemical shift to distinguish it at 0 ppm in the airspaces, 197 ppm in the lung tissue barrier and 211 ppm in the red blood cells (RBCs). ^{129}Xe transfer to the RBCs can be impaired in pulmonary diseases such as fibrosis or inflammation, which cause a thickening of the gas diffusion barrier and can be observed spectroscopically by comparing the ratio of the RBC peak to that of the tissue barrier peak (2). Details of the spectroscopy protocol can be found in reference (2). Briefly, spectra were acquired using a 1.05 ms 3-lobe sinc excitation pulse (3.8 kHz bandwidth), centered at 204 ppm to provide a 90° flip to the 197 ppm and 211 ppm resonances, while applying a ~0.15° flip to the airspace ^{129}Xe to provide a 0 ppm reference signal. The pulse thus simultaneously read and destroyed the dissolved ^{129}Xe signals and therefore, its repetition time (TR) set the time scale for replenishment. TR values of 11, 15, 20, 30, 40, 50, 75, 100, 125, 150, 175, and 200 ms were used and, for each TR value, the maximum number of spectra was acquired (19,14,11,9,7,6,5,3,2,2,2,2) during the 200 ms breath-hold. Spectra were accumulated over 40 breaths and averaged so that the entire series took 10 minutes to acquire. To ensure that dissolved ^{129}Xe signals reflected the replenishment time set by TR, the entire 1st breath of signals was discarded, and the first signal of each subsequent breath-hold period was discarded. The remaining spectra for each TR value were averaged in the time domain, then line broadened (25 Hz), Fourier transformed, baseline corrected and curve fit using functions written in MATLAB (The MathWorks, Natick, MA).

A typical dynamic spectroscopy series is shown in Figure 7 depicting the replenishment of ^{129}Xe in the tissue barrier and RBCs. The replenishment time constants can be used to infer mean tissue barrier thickness (25), while the ratio of the RBC to tissue barrier signal can serve as an indicator of global gas exchange efficiency. To extract these values the data were fit to a function discussed in the online supplemental material to reference (2). For our purposes, the critical observation is that the ^{129}Xe spectra and their dynamics could be probed with sufficient SNR using real-time ^{129}Xe delivery to permit accurate calculations of global gas exchange efficiency.

DISCUSSION

We have presented a method for real-time *in vivo* delivery of HP ^{129}Xe in rodents, which in its present form, is already useful for many aspects of our small animal imaging workflow — localizing, shimming, setting transmitter gains, frequency, and testing pulse sequences. Real-time ^{129}Xe MRI should also be valuable for investigations that require images or spectra to be acquired at multiple time points during a study. Finally, the availability of an on-demand *in vivo* ^{129}Xe signal source should be very powerful for characterizing ^{129}Xe spectral peaks and their dynamics. Since ^{129}Xe signal is continuously available, experiments requiring saturation and replenishment of the ^{129}Xe magnetization can now be contemplated (26).

Real-time delivery of HP ^{129}Xe should already be possible to implement in human subjects. We estimate the required HP ^{129}Xe mixture delivery rate for human subjects will be ~10 liters/min. This production rate is already achieved today with the next generation ^{129}Xe polarizers described by Ruset et al (27). This polarizer achieves ^{129}Xe polarization in excess of 50% and would therefore provide a further SNR increase.

The ultimate vision of real-time ^{129}Xe MRI will be to combine high polarization and high ^{129}Xe concentration. This would increase SNR by at least 100 compared to what we have demonstrated and permit an entirely new range of ^{129}Xe MRI experiments to become feasible, particularly those beyond the lung (26,28). In fact, the polarization system described by Ruset (27) already produces HP ^{129}Xe at the necessary rate to deliver fully

NIH-PA Author Manuscript

NIH-PA Author Manuscript

NIH-PA Author Manuscript

concentrated HP ^{129}Xe to a rat. However, this will require extracting the HP ^{129}Xe in real-time from the He and N_2 buffer gases and this remains a problem to be solved. Eventually, one could envision ventilation of even human subjects with highly concentrated real-time HP ^{129}Xe. Human Xe inhalation is limited by anesthetic considerations to <35% alveolar concentration (29) rather than the ~75% we use for animals. Therefore human studies would consume HP ^{129}Xe at a rate of ~3.5 l/min and likely require real-time recycling and re-polarization of the patient's exhaled ^{129}Xe to minimize xenon consumption. While this represents a considerable technical leap, the new clinical applications that will be made possible could be quite extraordinary.

Acknowledgments

We thank Sally Zimney for assistance in preparation of the manuscript and Ozgun Ataman for his help in obtaining the ^{129}Xe polarization data. This work was performed at the Duke Center for In Vivo Microscopy, an NCRR National Biomedical Technology Resource Center (P41 RR005959), NCI R24 CA092656), with additional support from The GEMI Fund 2005 and NHLBI R21-HL-087094.

References

1. Moller HE, Chen XJ, Saam B, Hagspiel KD, Johnson GA, Altes TA, de Lange EE, Kauczor HU. MRI of the lungs using hyperpolarized noble gases. Magn Reson Med. 2002; 47(6):1029–1051. [PubMed: 12111949]
2. Driehuys B, Cofer GP, Pollaro J, Boslego J, Hedlund LW, Johnson GA. Imaging alveolar capillary gas transfer using hyperpolarized 129Xe MRI. Proc Natl Acad Sci U S A. 2006; 103(48):18278–18283. [PubMed: 17101964]
3. Golman K, in't Zandt R, Thaning M. Real-time metabolic imaging. Proc Natl Acad Sci U S A. 2006; 103(30):11270–11275. [PubMed: 16837573]
4. Ardenkjaer-Larsen JH, Fridlund B, Gram A, Hansson G, Hansson L, Lerche MH, Servin R, Thaning M, Golman K. Increase in signal-to-noise ratio of >10,000 times in liquid-state NMR. Proc Nat Acad Sci. 2003; 100(18):10158–10163. [PubMed: 12930897]
5. Haake M, Pines A, Reimer JA, Seydoux R. Surface-enhanced NMR using continuous-flow laser-polarized xenon. J Am Chem Soc. 1997; 119(48):11711–11712.
6. Walker TG, Happer W. Spin-exchange optical pumping of noble-gas nuclei. Reviews of Modern Physics. 1997; 69(2):629–642.
7. Walker TG. Estimates of Spin-Exchange Parameters for Alkali-Metal Noble-Gas Pairs. Phys Rev A. 1989; 40(9):4959–4963. [PubMed: 9902753]
8. Jau YY, Kuzma NN, Happer W. Magnetic decoupling of ^{129}Xe-Rb and ^{129}Xe-Cs binary spin exchange. Phys Rev A. 2003; 67(2):022720.
9. Baranga ABA, Appelt S, Romalis MV, Erickson CJ, Young AR, Cates GD, Happer W. Polarization of He-3 by spin exchange with optically pumped Rb and K vapors. Phys Rev Lett. 1998; 80(13): 2801–2804.
10. Happer W, Miron E, Schaefer S, Schreiber D, van Wijngaarden WA, Zeng X. Polarization of the Nuclear Spins of Noble-Gas Atoms by Spin Exchange with Optically Pumped Alkali-Metal Atoms. Phys Rev A. 1984; 29(6):3092–3110.
11. Nelson IA, Walker TG. Rb-Xe spin relaxation in dilute Xe mixtures. Phys Rev A. 2001; 65(1): 012712.
12. Fink A, Baumer D, Brunner E. Production of hyperpolarized xenon in a static pump cell: Numerical simulations and experiments. Phys Rev A. 2005; 72(5)
13. Romalis MV, Miron E, Cates GD. Pressure broadening of Rb D-1 and D-2 lines by He-3, He-4, N-2, and Xe: Line cores and near wings. Phys Rev A. 1997; 56(6):4569–4578.
14. Driehuys B, Cates GD, Miron E, Sauer K, Walter DK, Happer W. High-volume production of laser-polarized Xe-129. Appl Phys Lett. 1996; 69(12):1668–1670.
15. Lindstedt SL. Pulmonary Transit-Time and Diffusing-Capacity in Mammals. Am J Physiol. 1984; 246(3):R384–R388. [PubMed: 6703093]

NIH-PA Author Manuscript

NIH-PA Author Manuscript

NIH-PA Author Manuscript

16. Chen BT, Brau AC, Johnson GA. Measurement of regional lung function in rats using hyperpolarized ^{3}helium dynamic MRI. Magn Reson Med. 2003; 49(1):78–88. [PubMed: 12509822]

17. Hedlund LW, Johnson GA. Mechanical Ventilation for Imaging the Small Animal Lung. ILAR Journal. 2002; 43(3):159–174. [PubMed: 12105383]

18. Volgyesi GA, Tremblay LN, Webster P, Zamel N, Slutsky AS. A new ventilator for monitoring lung mechanics in small animals. J Appl Physiol. 2000; 89(2):413–421. [PubMed: 10926621]

19. Jameson CJ, Jameson AK, Hwang JK. Nuclear-Spin Relaxation by Intermolecular Magnetic Dipole Coupling in the Gas-Phase - Xe-129 in Oxygen. J Chem Phys. 1988; 89(7):4074–4081.

20. Nelson, I.; Driehuys, B.; Kadlecek, S. Remote Calibration of Accurate Hyperpolarized Gas Polarimetry. 12th Annual Scientific Meeting, ISMRM; 2004. p. 1689

21. Kuzma NN, Patton B, Raman K, Happer W. Fast nuclear spin relaxation in hyperpolarized solid ^{129}Xe. Phys Rev Lett. 2002; 88(14):147602. [PubMed: 11955177]

22. Driehuys B, Walker JK, Pollaro J, Cofer GP, Mistry N, Schwartz DA, Johnson GA. 3He MRI in Mouse Models of Asthma. Magn Reson Med. 2007; 58(5):893–900. [PubMed: 17969115]

23. Zhao L, Mulkern R, Tseng CH, Williamson D, Patz S, Kraft R, Walsworth RL, Jolesz FA, Albert MS. Gradient-echo imaging considerations for hyperpolarized 129Xe MR. J Magn Reson B. 1996; 113(2):179–183.

24. Ruppert K, Brookeman JR, Hagspiel KD, Driehuys B, Mugler JP. NMR of hyperpolarized 129Xe in the canine chest: spectral dynamics during a breath-hold. NMR Biomed. 2000; 13(4):220–228. [PubMed: 10867700]

25. Mansson S, Wolber J, Driehuys B, Wollmer P, Golman K. Characterization of diffusing capacity and perfusion of the rat lung in a lipopolysaccaride disease model using hyperpolarized Xe-129. Magn Reson Med. 2003; 50(6):1170–1179. [PubMed: 14648564]

26. Schroder L, Lowery TJ, Hilty C, Wemmer DE, Pines A. Molecular imaging using a targeted magnetic resonance hyperpolarized biosensor. Science. 2006; 314(5798):446–449. [PubMed: 17053143]

27. Ruset IC, Ketel S, Hersman FW. Optical pumping system design for large production of hyperpolarized Xe-129. Phys Rev Lett. 2006; 96(5):053002. [PubMed: 16486926]

28. Swanson SD, Rosen MS, Coulter KP, Welsh RC, Chupp TE. Distribution and dynamics of laser-polarized 129Xe magnetization in vivo. Magn Reson Med. 1999; 42(6):1137–1145. [PubMed: 10571936]

29. Muradian, I.; Butler, JP.; Hrovat, MI.; Topulos, GP.; Hersman, E.; Frederick, S.; Covrig, S.; Ruset, IC.; Ketel, S.; Hersman, FW.; Patz, S. Human Regional Pulmonary Gas Exchange with Xenon Polarization Transfer (XTC). 15th Annual Scientific Meeting, ISMRM; 2007. p. 454

NIH-PA Author Manuscript

NIH-PA Author Manuscript

NIH-PA Author Manuscript

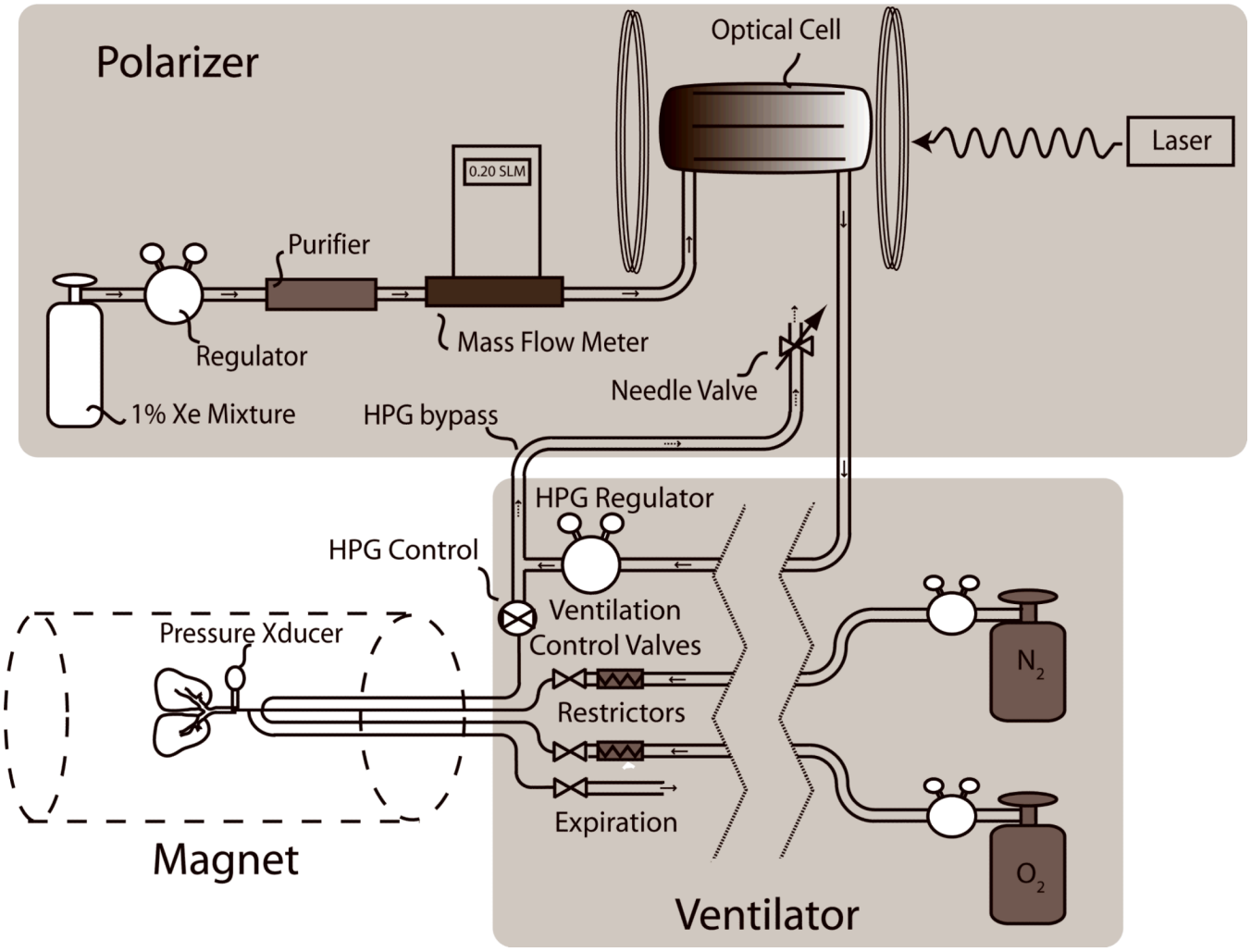

Figure 1.

^{129}Xe polarizer with modifications needed for real-time *in vivo* delivery of HP ^{129}Xe. The key modification was to remove the cryogenic accumulation stage of a conventional polarizer and to introduce an HP-gas-compatible Teflon regulator to reduce the pressure to physiologic levels to permit direct delivery of the HP ^{129}Xe mixture to the animal. The inspiration of the ^{129}Xe mixture is controlled by an HP gas-compatible pneumatic Teflon valve.

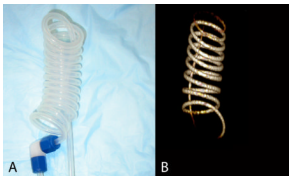

Figure 2.

A. Teflon (PFA) spiral phantom used for in vitro ^{129}Xe polarization characterization studies and pulse sequence testing. B. An image of ^{129}Xe flowing through the phantom at 0.2 SLM was acquired with $(0.94\text{mm})^3$ isotropic resolution and shows the utility of real-time ^{129}Xe MRI for pulse sequence testing.

NIH-PA Author Manuscript NIH-PA Author Manuscript NIH-PA Author Manuscript

NIH-PA Author Manuscript

NIH-PA Author Manuscript

NIH-PA Author Manuscript

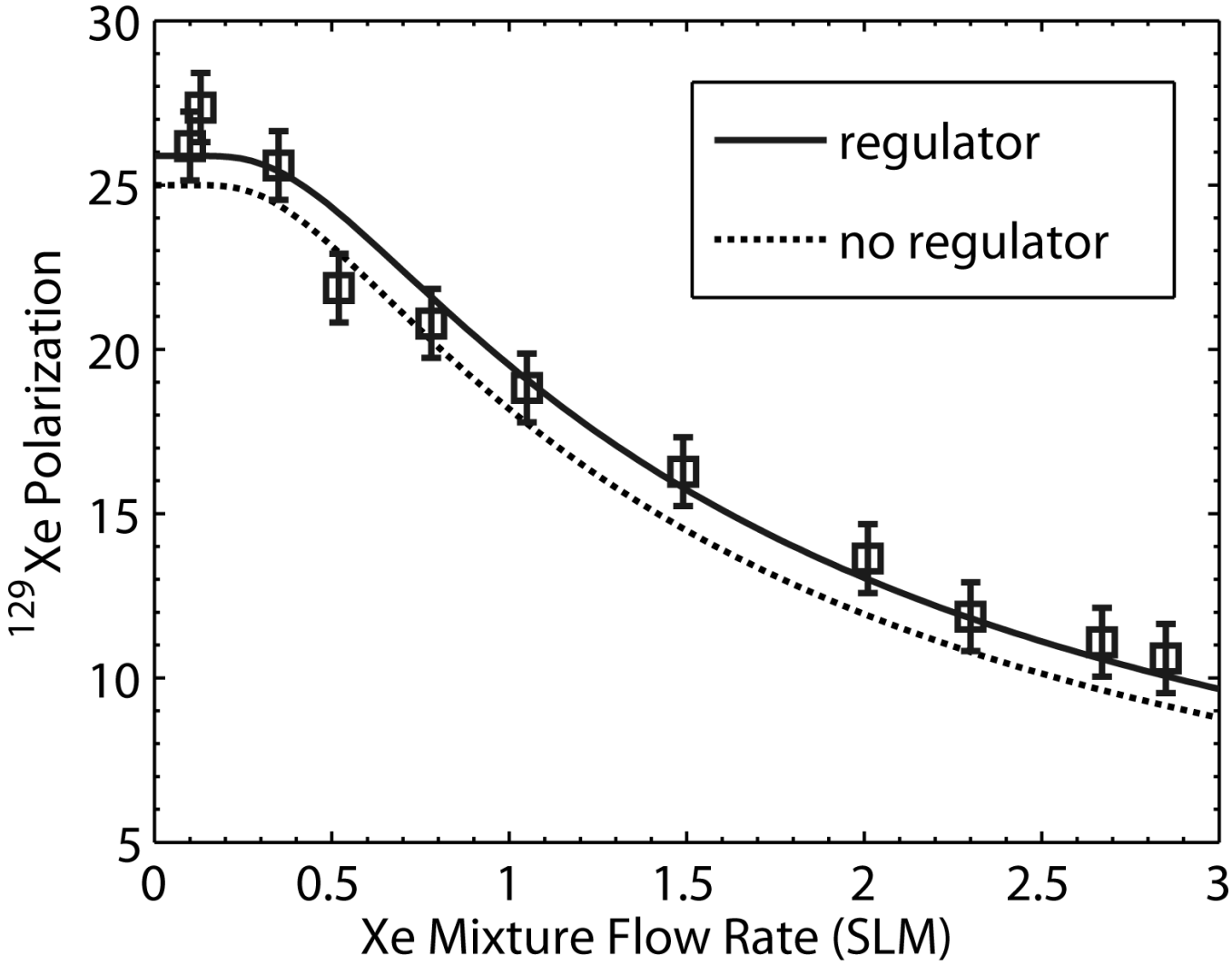

Figure 3.
^{129}Xe polarization as a function of flow rate taken with and without the Teflon pressure regulator inserted. These data indicate that, to within error, the ^{129}Xe polarization is unaffected by flowing through the regulator and that the Xe mixture can be delivered to the animal at 25% polarization.

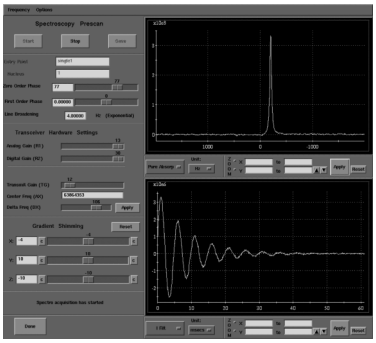

Figure 4.
Screen capture of the pre-scan window of our GE EXCITE 12 console during real-time *in vivo* HP ^{129}Xe delivery to a rat. The signal acquisition is gated to the rat's ventilation and is repeated every second, and thus can be used for shimming, setting frequency, and determining transmitter gain.

NIH-PA Author Manuscript NIH-PA Author Manuscript NIH-PA Author Manuscript

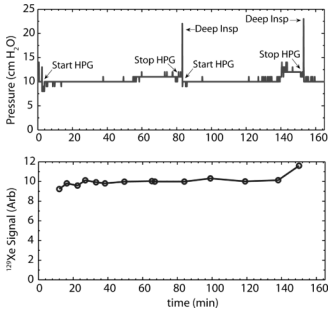

Figure 5.

Stability of airway pressure (top) and ^{129}Xe signal (bottom) over the course of 160 minutes of continuous ^{129}Xe ventilation. HP ^{129}Xe is started at t=4 minutes and the PIP is adjusted. The pressure remains constant with only a very slight rise over the course of 80 minutes. The HP ^{129}Xe is stopped, the animal is given a deep inspiration to reset its lungs and HP gas is started again. The pressure again remains stable until about t=140 min when it begins to rise slightly. HP ^{129}Xe is stopped and the animal is given another resetting breath. The bottom plot shows that the ^{129}Xe signal is very stable over time and tracks the inspiratory pressure, only experiencing a final rise at about 150 min.

NIH-PA Author Manuscript NIH-PA Author Manuscript NIH-PA Author Manuscript

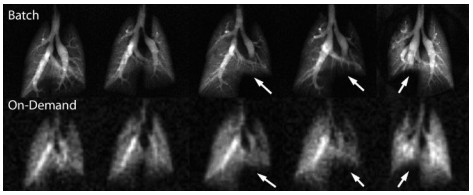

Figure 6.
Representative images from five rats acquired using both conventional delivery of fully concentrated ^{129}Xe (top row) or real-time ^{129}Xe delivery bottom row. The three right-most animals each had restricted ventilation in one lung caused by fibrotic injury. This altered the ventilation (arrows) and is readily apparent even on the real-time ^{129}Xe scans.

NIH-PA Author Manuscript
NIH-PA Author Manuscript
NIH-PA Author Manuscript

NIH-PA Author Manuscript
NIH-PA Author Manuscript
NIH-PA Author Manuscript

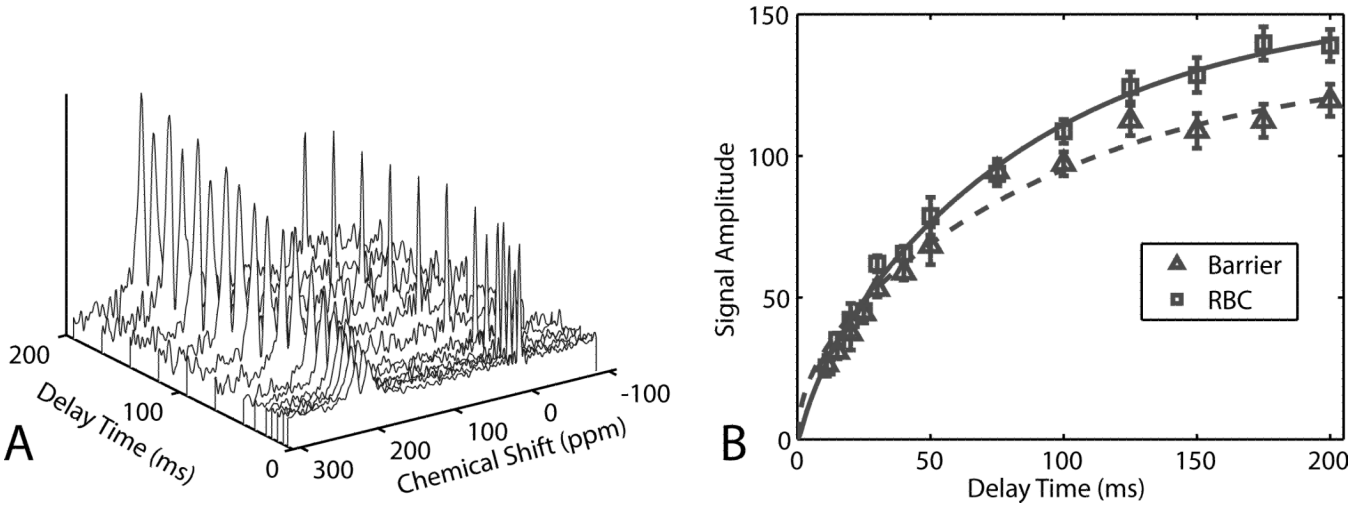

Figure 7.

A. ^{129}Xe dynamic spectra acquired using continuous ^{129}Xe delivery. Each spectrum was acquired at end-inspiration and was averaged over 40 breaths. **B.** From the spectra at different delay times, the replenishment of ^{129}Xe in RBCs and pulmonary tissues could be readily extracted. Such spectroscopy is useful to quickly assess gas exchange efficiency in rodent models pulmonary disease.